sciendo

Civil and Environmental Engineering
Vol. 20, Issue 2, 699-710, DOI: 10.2478/cee-2024-0052

NUMERICAL MODELING OF LOCAL SCOUR DEPTH AT NON-UNIFORM PIERS

Ahmed A. DAKHEEL[1,*], Abaas J. ISMAEEL [2], Jamal S. MAKKI [2]

[1] University of Thi-Qar, Thi-Qar, Iraq.
[2] Civil Engineering Department, College of Engineering, University of Thi-Qar, Thi-Qar, Iraq.
[*] corresponding author: msc_ahmed@utq.edu.iq

Abstract

One of the most dangerous issues in river engineering is erosion brought on by the flow around bridge piers, which causes failure. As a result, simulating scouring is a crucial technique for assessing the likelihood of scour-related bridge failure. The scour depth surrounding hydraulic structures (non-uniform piers) was investigated using various computational and laboratory models. This study examines the efficacy of the computational fluid dynamics (CFD) model in generating simulations of the scour depth along a bridge pier via the Flow3D software (version 10.1.1.3). k-ε model is built to more accurately consider the generation of turbulent kinetic energy and the anisotropic characteristics of the turbulence. The model's calibration and verification are assessed using statistical metrics (Root Mean Square Error (RMSE), Mean Absolute Error (MAE), and coefficient of determination (R2)). Based on the statistical criteria, it may be concluded that the model's results were promising because the discrepancy between the numerical and experimental models is negligible. The Froude number has been demonstrated to be a crucial factor that must be considered during the construction of piers, since reducing it will result in a decrease in longitudinal velocity and turbulent kinetic energy. Also, the Flow-3D program accurately reproduces the scour depth, flow, and velocity near the pier.

Keywords:

Scour;
Non-uniform piers;
Bridge;
CFD;
Flow-3D.

1 Introduction

Bridges are vital elements of the transportation infrastructure, and their malfunctioning can lead to significant economic and human casualties. The main reasons for bridge failure are overloading, collision, and foundation scour [1]. Consequently, there is a growing need to find the most efficient design that offers superior performance and capabilities while minimizing its influence on the environment [2-8]. Scour constitutes one of the adverse environmental consequences associated with artificial structures. Scour is a phenomenon characterized by sediment erosion from the river's bed and margins, along piers and buttresses, and at the base and borders of the river. This occurs due to the increased speed of water flow and its erosive effects [9-11]. Erosion surrounding bridge piers occurs through overflow periods, often caused by ripples [12-13]. Several research publications have thoroughly examined the scouring phenomenon near non-uniform Piers [14-15]. The aforementioned research findings established, as depicted in Figure 1, that the scour is brought about by elevated shear stresses generated by discharge acceleration near the pier.

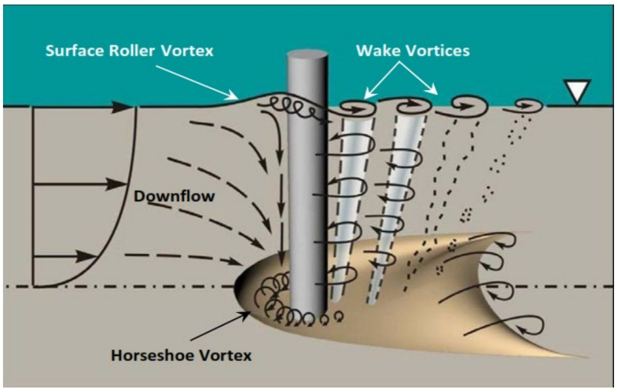

Fig. 1: Flow Features Forming the Flow Field Around Cylindrical Pier [16].

A substantial down-flow force on the face of the pier is an additional factor. With a circular pier cross-section, the horseshoe vortex is initially tiny and susceptible, but its dimensions and forces develop as the scour hole expands and moves downward [17]. The primary cause of the bridge's breakdown was determined to be pier and abutment degradation caused by the scouring of the river's base [18]. According to the Federal Highway Administration, scouring causes sixty percent of all bridge failures in the U.S. [19], and around 60 bridges fall yearly [20]. Moreover, assessments unveiled that failure, according to information collected from other countries, natural disasters are the most probable cause of the bridge collapse [20].

Experimental models were frequently used to examine a variety of subjects [22-24]. Numerous research were undertaken to address the scour problems related to hydraulic structures. Ataie-Ashtiani et al.(2010) [25] conducted seventy tests with rectangular piers placed on piles or caissons; the results indicated that the pile cap or caisson prevented bed scour and delayed the onset of the cleansing process when it was positioned at bed level. Veerappadevaru et al. (2011) [26] proposed a technique to forecast the stable erosion depth around caisson piers using the power principle of the central vortex. The caisson's width was double that of the cylindrical pier. Thorat et al. (2012) [27] conducted an empirical study on the scour of sediment near a circular pier, a non-uniform bridge pier consisting of a circular pier built atop a bigger diameter circular footing. Several geometries of compound piers were examined in the experiment under conditions of pristine water scour using both uniform and non-uniform sediments. In relation to the initial bed level, the compound pier was situated at three distinct levels: the superior level of the foundation at bed level, the superior level below bed level, and the superior level above bed level. Significant erosion has been observed to occur at foundation levels above the initial bed level, with a subsequent decrease in erosion at the bed level and below. Research has demonstrated that non-uniform sediment experiences reduced scouring in comparison to uniform sediment.

The rising capabilities of computational fluid dynamics (CFD) software have also improved the modeling technique for scouring, which is similar to planning an experiment. FLOW 3D is an application of CFD. The equations for multi-physics flow problems can be solved using computational fluid dynamics (CFD) software [28]. Additionally, it contains multi-scale multi-physics flow models and numerical methods for solving equations relating to fluid motion. A sequence of scientific investigations was conducted using FLOW 3D to examine the erosion caused by scouring. M. Ghasemi et al. [29] tested FLOW 3D's capacity to simulate scour depth under various noncohesive sediment velocity conditions. I.S.P. Mendonça et al. [30] studied erosion depth around a cylindrical pier caused by clear water scour using FLOW 3D. H.K. Jalal et al. [31] used FLOW 3D to simulate the impact of detritus on the greatest depth of scour holes to bridge piers. M. Sadat Helbar et al. [32] utilized the FLOW 3D model to demonstrate the program's proficiency in simulating reservoir flushing using laboratory results.

As previously stated, scour is an essential factor that causes bridge collapses worldwide by removing the river's bed material. Hence, the article's objective is to utilize the CFD model, namely FLOW 3D, to examine the effects of critical factors on the erosion of an oblong pier with a foundation. Additionally, the study intends to validate the effectiveness of FLOW 3D in simulating the erosion surrounding hydraulic structures, particularly non-uniform piers.

2 Materials and Methods

2.1 Experimental Tests

The experimental model was performed in the fluid laboratory of the Civil Engineering Department of the College of Engineering at the University of Basra [33]. It occurred in a flume with a closed system of water recirculating. The length of the flume is 5.72 m, the width is 0.615m, and the height is 0.97m. Figure 2 shows the full details of the flume. In the laboratory, a sand bed with a consistent grain size was utilized, with a median size of 0.4 mm; the following conditions were utilized in the experiments: steady flow clear water, plain bed, and subcritical flow. The test occurred for types of non-uniform piers; a non-uniform Pier is a uniform Pier placed on footing. The shape of the piers was oblong, as shown in Figure 3, and the shape of the foundation was oblong, as shown in Figure 4. The tests occurred with a pier width of (4 cm), height (17cm), width of footing (6cm) and height (8cm). (Pier with footing) models are fixed in the middle of the channel.

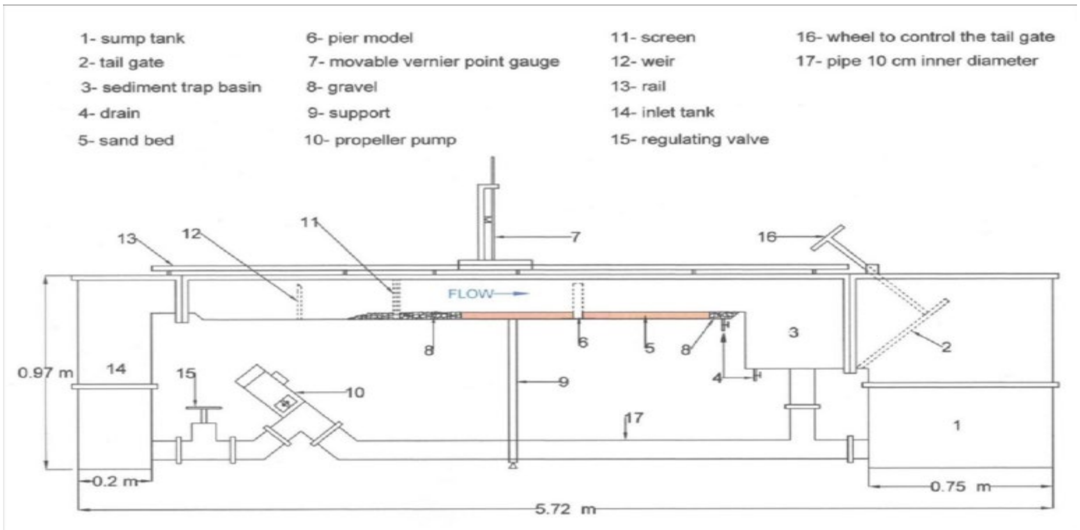

Fig. 2: Schematic Diagram of the Laboratory Flume [33].

Fig. 3: Pier shape [33].

Fig. 4: Foundation shape [33].

2.2 FLOW 3D Model

Using the FLOW 3D software (version 10.1.1.3), the three-dimensional sediment scours model is intended to simulate local scours around the bridge pier. Fluid flow is appropriately coupled with the FLOW 3D system to convey numerous non-cohesive species, deposition, bedload, and suspended loads. The statistical metrics used to assess the disparity between the measured and computed values include the Root Mean Square Error (RMSE), Mean Absolute Error (MAE), and coefficient of determination (R^2).

2.2.1 Governing Equations

The hydrodynamic Model is the foundation for modeling sediment movement, particle monitoring, and morphological bed updating. Hydrodynamic models are utilized to solve fluid motion governing equations [34].

2.2.1.1 Hydrodynamic Model (HD)

HD simulates the water level fluctuations and fluxes in estuaries, lakes, and rivers in response to various forcing functions. Model equations include continuity and momentum equations. The local continuity equation is written in Eq. 1, and momentum equations are written in Eq. 2 to 4 [35].

$$\frac{\partial u}{\partial x}+\frac{\partial v}{\partial y}+\frac{\partial w}{\partial z}=0 \quad (1)$$

$$\rho\left(\frac{\partial u}{\partial t}+u\frac{\partial u}{\partial x}+v\frac{\partial u}{\partial y}+w\frac{\partial u}{\partial z}\right)=-\frac{\partial p}{\partial x}+\rho g_x+\mu\left(\frac{\partial^2 u}{\partial x^2}+\frac{\partial^2 u}{\partial y^2}+\frac{\partial^2 u}{\partial z^2}\right) \quad (2)$$

$$\rho\left(\frac{\partial v}{\partial t}+u\frac{\partial v}{\partial x}+v\frac{\partial v}{\partial y}+w\frac{\partial v}{\partial z}\right)=-\frac{\partial p}{\partial y}+\rho g_y+\mu\left(\frac{\partial^2 v}{\partial x^2}+\frac{\partial^2 v}{\partial y^2}+\frac{\partial^2 v}{\partial z^2}\right) \quad (3)$$

$$\rho\left(\frac{\partial w}{\partial t}+u\frac{\partial w}{\partial x}+v\frac{\partial w}{\partial y}+w\frac{\partial w}{\partial z}\right)=-\frac{\partial p}{\partial z}+\rho g_z+\mu\left(\frac{\partial^2 w}{\partial x^2}+\frac{\partial^2 w}{\partial y^2}+\frac{\partial^2 w}{\partial z^2}\right) \quad (4)$$

Where:
μ - dynamic viscosity of water (M/TL),
p - pressure (F/L^2),
g - gravitational acceleration (L/T^2),
t - time (T),
ρ − density (M/L^3).

The three orthogonal components of the instantaneous velocity field in Cartesian coordinates (x, y, z) are denoted by (u, v, w). The z-axis has a positive direction that is oriented upwards.

2.2.1.2 Sediment Transport Model (ST)

The sediment transport formulae rely on the advection-dispersion calculations of the hydrodynamic model. Advection and dispersion are the terms used to describe the motion of particles in a fluid. Particle motion and the average fluid flow is known as the advective component of mass transfer. Dispersion is when particles move randomly in a fluid because of a difference in velocity, resulting in turbulent dispersion. Moreover, turbulent diffusion occurs when there is a gradient in the suspended material [36]. Equation 5 provides a comprehensive description of the sediment transport[37]:

$$\frac{\partial \bar{c}}{\partial t}+u\frac{\partial \bar{c}}{\partial x}+v\frac{\partial \bar{c}}{\partial y}=\frac{1}{h}\frac{\partial}{\partial x}\left(hD_x\frac{\partial \bar{c}}{\partial x}\right)+\frac{1}{h}\frac{\partial}{\partial y}\left(hD_y\frac{\partial \bar{c}}{\partial y}\right)+QC_L\frac{1}{h}-S \quad (5)$$

Where:
$\bar{c}$ - Depth averaged concentration,
u and v - Depth averaged flow velocities,
D_x and D_y - Dispersion coefficients,
h - Water depth,
Q - Source discharge per unit horizontal area,
C_L - Concentration of the source discharge,
S - Deposition/erosion term.

2.2.2 Developing Models

CFD (Computational Fluid Dynamics) model was implemented in Flow-3D to simulate a rectangular channel measuring 4.2m in length and 0.615 m in cross-sectional width. The oblong pier with dimensions of 4 cm width and length of 17 cm was used. It was placed on an oblong foundation with a 6 cm width and length of 8 cm.

The particle measured 0.0004 m in diameter and 2650 kg/m3 in density. It possessed a drag coefficient of 0.5 and a critical shield number of 0.05. k–ε model is employed to more effectively consider the generation of turbulent kinetic energy and the anisotropic characteristics of the turbulence. The mesh consisted of 50,000 cells, which were accurately aligned with the model geometry, as seen in Figures 5 and 6. Besides, the mesh intensification will occur around the pier for more acceptable resolutions.

One of the most critical factors determining the accuracy of models is the mesh design, which depends on the volume, number, and concentrated position of cells. Additionally, it might shorten simulation time. The elevation Z of the foundation's top is determined relative to the initial bed level. A foundation is deemed positive when its top is positioned below the initial bed level and negative when it is situated above. Three distinct levels of Z/D = 0, + 0.25, and -0.25 were employed in constructing the foundation.

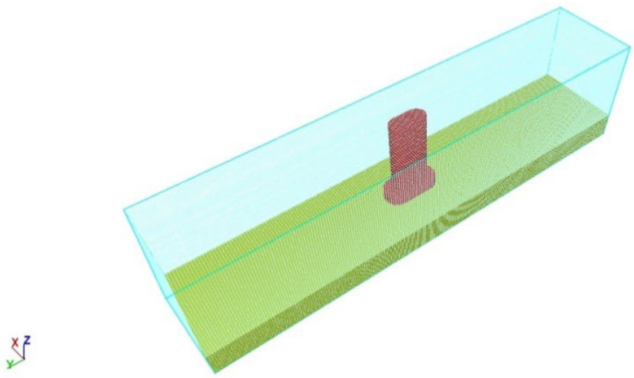

Fig. 5: Displays the 3D meshing of the channel.

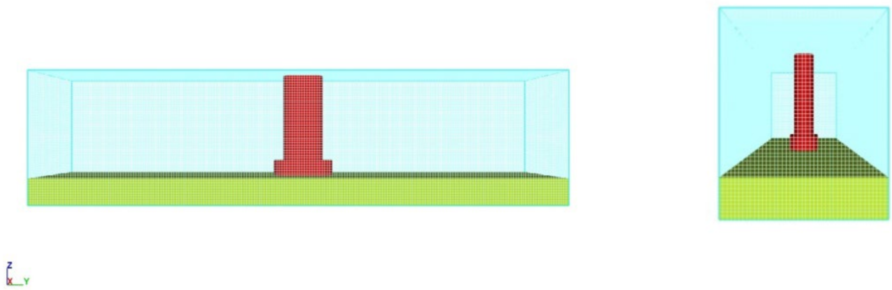

Fig. 6: Meshing from different angles.

2.2.3 Initial & Boundary Conditions

Selecting suitable boundary conditions for the hydraulic model is paramount in numerical simulation. Therefore, the numerical model should match the problem's physical requirements. Therefore, proper consideration should be given to the boundary conditions and several vital factors while setting up the numerical Model because they directly impact the outcomes. Based on the experimental investigation, it was believed that the velocity in this study would be under live bed settings.

The boundary conditions were provided, as seen in Figure 7. For the inlet border, the discharge rate is chosen in Y min. Water is moving at 0.21 m/s in the inflow and outflowing at Y max. The water is 20 cm deep. The modal conditions determine the pressure and velocity at the inlet border. For X min and X max, the right and left sides are regarded as walls, Z min is the bottom wall, and Z max has a defined specified pressure on the upper border to simulate open channel conditions. To simulate the scour of an oblong pier, the Model's boundary conditions, the geometry of the flume, and its plane meshing are illustrated in Figure 7.

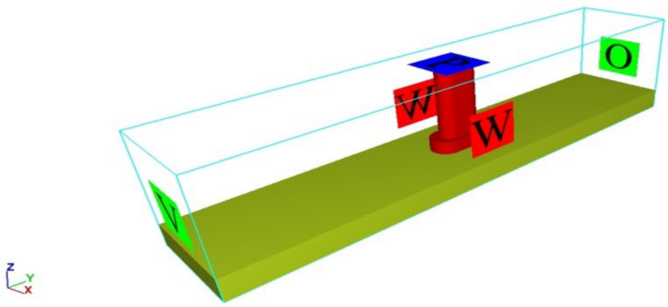

Fig. 7: Boundaries for the numerical Model.

A fluid region in a sediment box technique was utilized for initial conditions to have saturated sediment and keep material from quickly eroding and washing out of the channel due to channel flow.

3 Results and Discussion

To assess the efficiency of the FLOW-3D model and examine the scour depth and velocity at the pier, a numerical simulation was conducted using parameters that closely resembled those in the experimental Model. By contrasting the results with the practical test, the impact of the scour on the riverbed surrounding the oblong bridge pier with the foundation oblong was also examined. The comparison between simulated and measured scour depth around oblong pier was referred to in Figure 8, with RMSE, MAE, and R^2 shown in Table 1.

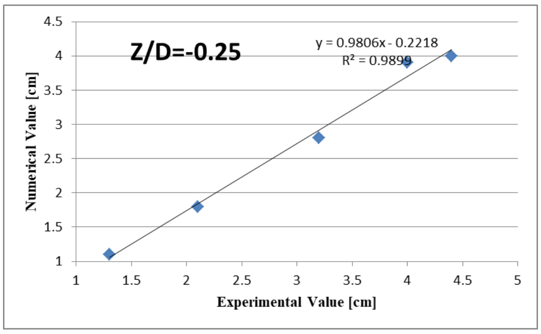

(a)The foundation level below bed level.

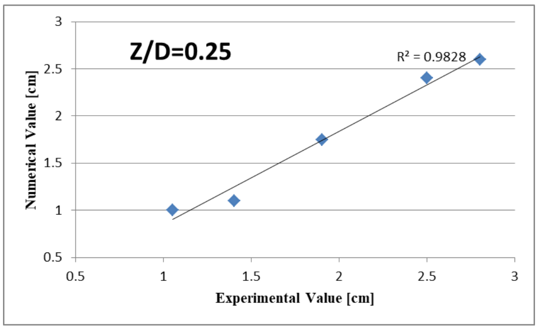

(b) The foundation level above bed level.

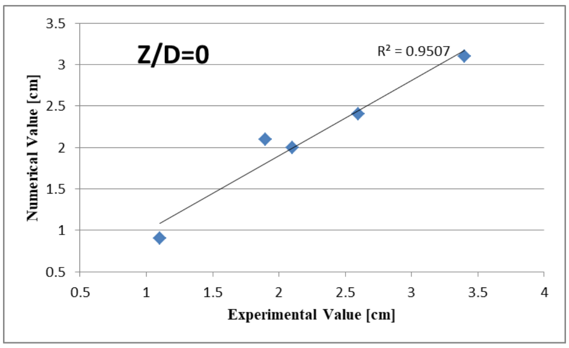

(c) The foundation level at the bed level

Fig. 8: The calibration and the verification values of scour depth around Oblong Pier.

Table 1: RMSE, MAE, and R^2 of scour depth during the calibration and the verification period.

Three different levels of foundation		RMSE	MAE	R^2
calibration	Z/D=-0.25	0.3033	0.28	0.989
	Z/D=0.25	0.2097	0.20	0.982
verification	Z/D=0	0.1817	0.16	0.950

3.1 The Physics Study

After the verification of Flow-3D program results, it has been used to perform a physic variables study on the affecting the scour process around piers. These parameters are:
• Reynold's Number (Re).
• Froude number (Fr).

3.1.1 Reynold's Number (Re)

Reynolds number (Re) (Eq.6) value is a measure of flow turbulence and indicates of eddies zones. Reynolds number grows, it is clear that the scour depth will also increase, taking into account the significant impact of flow velocity [38-39]. Scour depth versus Reynolds number yielded intricate non-linear relationships in three various levels of foundation, show in Figure 9.

$$\mathrm{Re} = \frac{\mathrm{V\,Dp}}{\mathrm{v}} \tag{6}$$

Where:
V - Flow velocity,
Dp - Pier diameter,
v - Kinematic viscosity.

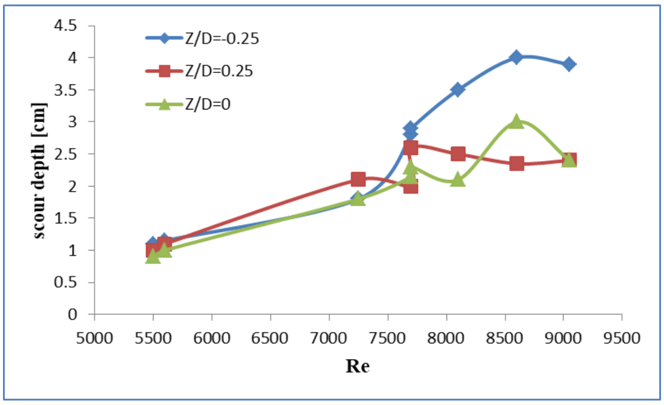

Fig. 9: Variation of scour depth with Reynolds number.

3.1.2 Froude number (Fr)

Table 2 shows the relationship between Froude Number Eq.7, the maximum values of the longitudinal velocity, bed shear velocity, turbulent kinetic energy, turbulent dissipation, and scour depth for the three cases of foundation.

$$\mathrm{Fr} = \frac{\mathrm{V}}{\sqrt{\mathrm{gH}}} \tag{7}$$

Where:
V - Flow velocity,
g - Gravitational acceleration,

H - Depth of flow.

To elucidate the effect of the Froude number three different values (0.490, 0.436, and 0.386) have been studied. All Fr values are less than 1, which means that the flow is subcritical.

The results show the changes in the longitudinal and bed shear velocities with changing Froude numbers.

From the result; it is so obvious that flow patterns and velocity values are sensitive to the Froude number. That means reducing the Froude number will reduce the rate of turbulent energy dissipation, the longitudinal velocity, bed shear velocity, and turbulent kinetic energy. This finding can be considered as an indicator of the scour process formation. Therefore increasing the Froude number causes the formation of more eddies and enhances their strength and, consequently, these areas are expected to have more erosion.

Table 2: Comparison between the calculated values of maximum velocity and the other terms for the three cases of Froude number.

Three different levels of foundation	Froude number	Maximum velocity [m/sec]	Maximum bed shear velocity [m/sec]	Turbulent kinetic energy [m^2/s^2]	Turbulent dissipation [m^2/s^3]	Maximum scour around the pier [cm]
Z/D=-0.25	0.386	0.236	0.0166	0.001187	0.00634	2.9
	0.436	0.257	0.0210	0.001232	0.01270	3.4
	0.490	0.315	0.0224	0.001558	0.06410	4
Z/D=0.25	0.386	0.223	0.0157	0.001056	0.00413	2.1
	0.436	0.251	0.0189	0.001195	0.01183	2.35
	0.490	0.296	0.0211	0.001532	0.06390	2.6
Z/D=0	0.386	0.241	0.0188	0.001202	0.00748	2.16
	0.436	0.262	0.0215	0.001251	0.01394	2.3
	0.490	0.340	0.0232	0.001642	0.07551	3.1

3.2 Velocity and Flow near the pier

Pier in the channel serves as an impediment to the flow of water. Flow was constant at a specified velocity of 0.21 m/s till it reached the pier. Additionally, Figure 10 shows that the velocity increases as the water approaches the pier's two sides. As shown in Figure 11, flow reversion occurs in the scour crater, as indicated by the blue vectors oriented in the reverse direction. The reversal of flow creates a vortex that starts at the bottom of the pier as a result of downward movement.

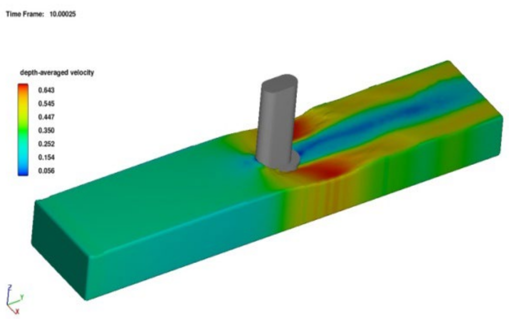

Fig. 10: 3D average flow velocity.

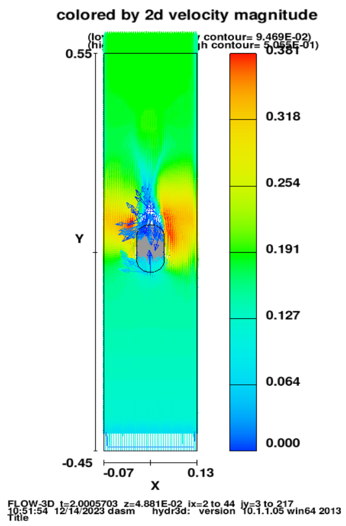

Fig. 11: 2D average flow velocity with vectors around the pier.

Furthermore, as illustrated in Figure 12, the velocity exhibits a progressive decline as it nears the channel bed. Specifically, it descends progressively at the front of the pier and does the same at the rear. Due to the differential in pressure caused by this, a vortex forms around the pier, intensifying on its front side.

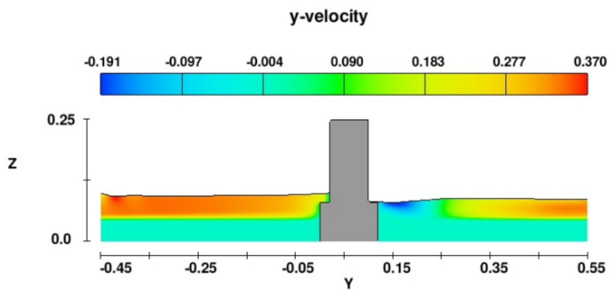

Fig. 12: Numerical model of a pier that compares the front and posterior velocities.

3.3 Simulated Scour Depth

The highest scour depth in the simulation model was approximately 4 cm, compared to 4.4 cm for the experimental Model when Z/D=-0.25, 2.6cm for the simulated Model compared to 2.8 cm for the experimental Model when Z/D=0.25 and at Z/D=0 the highest scour depth 3.1 cm for the simulated Model compared to 3.4 cm concerning the experimental paradigm. The findings indicated that the experimental and numerical models came near the utmost scour depth. Figures 13 and 14 illustrates the many ways in which the scour pit is built and sediments are deposited near the pier. The scouring simulation indicates that the most incredible depth occurs on both sides of the pier, although slightly less right in front of it. As a result, the computational fluid dynamics (CFD) results yield a lower evaluation than the physical Model.

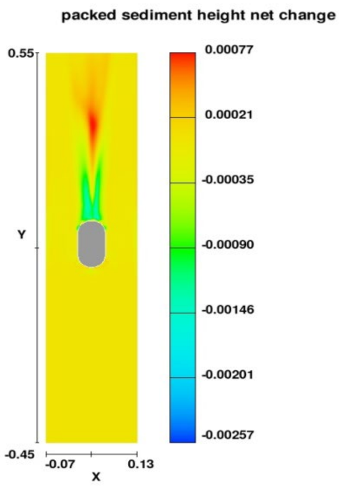

Fig. 13: Scour depth near the pier for the Numerical Model.

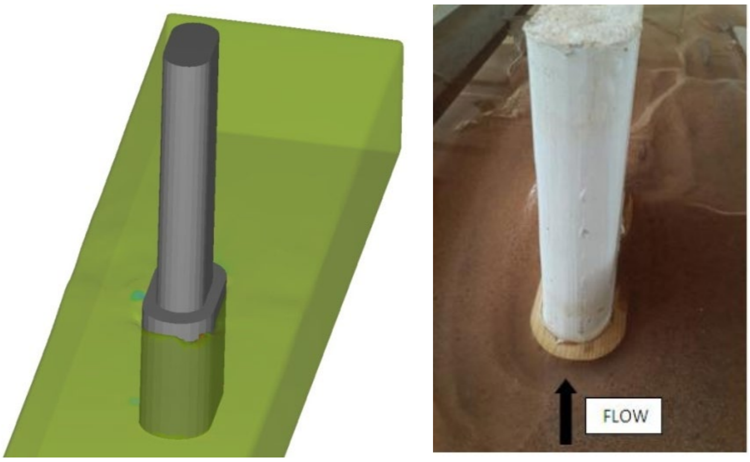

Fig. 14: Formation of the experimental Model and CFD channel beds following a full-time run (The foundation level below bed level).

3.4 Evolution of Scour Depth throughout Time

Figure 15 illustrates the progression of the maximum scour depth over time for both the experimental and numerical models, specifically after two hours. The FLOW-3D model's maximum scour depth was 4 cm, while the experimental Model's maximum scour depth was 4.4 cm when the foundation level was below bed level. The outcomes of the numerical model and the experimental model were in agreement. Numerical test was over when the scour rate dropped to about 5% of the pie's diameter. The Model has reached the equilibrium stage.

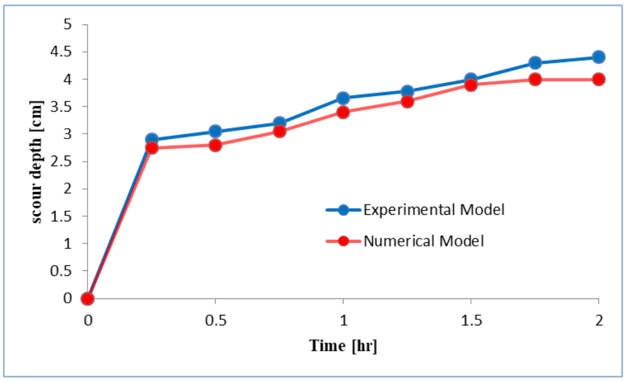

Fig. 15: Evolution of the greatest scour depth over time.

4 Conclusions

Scrubbing in stream channels near bridge foundations frequently results in bridge failure. Therefore, civil engineers must ascertain the utmost scour depth. This research selects an oblong bridge pier with the foundation oblong from an experimental study by Saja Ibrahim Ahmed, 2019, to simulate the scour behaviour using the FLOW3D program. The Model has been calibrated under identical conditions to ensure the precision of the outcomes. Additionally, the FLOW3D program displayed a 9% inaccuracy compared to the experimental Model. The following are the study's primary outcomes:

1) The Flow-3D Model is capable of accurately simulating hydrodynamic flow and sediment transport. The experimental Model and computed results exhibited a strong agreement in terms of flow velocity and scour depth. Therefore, the Flow-3D software is a dependable tool for studying bridge pier scour.

2) One of the influencing aspects in the modelling process is the mesh, which may impact the accuracy of the results.

3) The study found that there are intricate, non-linear connections between the scour depth and the Reynolds number. Additionally, the flow patterns and velocity values are highly responsive to variations in the Froude number.

4) The numerical model findings for the oblong pier yielded a minor estimation of the scour depth at the front of the pier compared to the experimental results obtained under identical conditions.

5) The cross-sectional form and flow characteristics determine how well the Model can reproduce the scour shape.

References

[1] RICHARDSON, E.V. – DAVIS, S.R.: Evaluating Scour at Bridges. Federal Highway Administration, 2001, 4th edition, FHWA-NHI-01-001.

[2] KASHANI, A.R. – CAMP, C.V. – ROSTAMIAN, M. – AZIZI, K. – GANDOMI, A.H.: Population-Based Optimization In Structural Engineering: A review, Artif. Intell. Rev., 2022, Vol. 55, pp. 345–452.

[3] KASHANI, A.R. – CAMP, C.V. – AZIZI, K. – ROSTAMIAN, M.: Multiobjective Optimization of Mechanically Stabilized Earth Retaining Wall Using Evolutionary Algorithms, Int. J. Numer Anal Methods Geomech, 2022, Vol. 46, pp. 1433–1465.

[4] AKHANI, M. – KASHANI, A.R. – MOUSAVI, M. – GANDOMI, A.H.: A Hybrid Computational Intelligence Approach To Predict Spectral Acceleration, Measurement: Journal Of The International Measurement Confederation, 2019, Vol. 138, pp. 578–589.

[5] GANDOMI, M. – KASHANI, A.R. – FARHADI, A. – AKHANI, M. – GANDOMI, A.H.: Spectral Acceleration Prediction Using Genetic Programming Based Approaches, Appl. Soft Computer, 2021, Vol. 106(C) pp. 13.

[6] KASHANI, A.R. – AKHANI, M. – CAMP, C.V. – GANDOMI, A.H.: A Neural Network to Predict Spectral Acceleration, Basics of Computational Geophysics, ELSEVIER, 2021, pp. 335–349.

[7] AZARI, B. – TABESH, M.: Optimal Design of Storm water Collection Networks Considering Hydraulic Performance and Bmps, International Journal of Environmental Research, 2018, Vol. 12, pp. 585–596.

[8] AZARI, B. – TABESH, M.: Urban Storm Water Drainage System Optimization Using A Sustainability Index And Lid/Bmps, Sustainable Cities and Society, 2022, Vol. 76, pp. 103-500.

[9] BREUSERS, H. – NICOLLET, G. – SHEN, H.: Local Scour around Cylindrical Piers, Journal of Hydraulic Research, 1977, Vol. 15, pp. 211–252.

[10] KHWAIRAKPAM, P. – MAZUMDAR, A.: Local Scour around Hydraulic Structures, International Journal of Recent Trends in Engineering, 2009, Vol. 59.

[11] SHAKIR, A. A. – GUNAL, M.: Artificial Neural Network for Estimation of Local Scour Depth around Bridge Piers, Archives of Hydro-Engineering and Environmental Mechanics, 2021, Vol. 68.

[12] LINK, O. – CASTILLO, C. – PIZARRO, A. – ROJAS, A. – ETTMER, B. – ESCAURIAZA, C. – MANFREDA, S.: A Model of Bridge Pier Scour During flood Waves, Journal Of Hydraulic Research, 2017, Vol. 55, pp. 310–323.

[13] HAGER, W.H. – UNGER, J.: Bridge Pier Scour under Flood Waves, Journal of Hydraulic Engineering, 2010, Vol. 136, pp. 842–847.

[14] MELVILLE, B.W. – RAUDKIVI, A.J.: Flow Characteristics in Local Scour at Bridge Piers, Journal of Hydraulic Research, 1977, Vol. 15, pp. 373–380.

[15] CHIEW, Y.M. – MELVILLE, B.W.: Local Scour around Bridge Piers, Journal of Hydraulic Research, 1987, Vol. 25, pp. 15–26.

[16] ARNESON, L.A. – ZEVENBERGEN, L.W. – LAGASSE, P.F – CLOPPER, P.E.: Evaluating Scour at Bridges, Hydraulic Engineering Circular, 2012, No. 18, 5th Edition, Fhwa-Hif-12-003.

[17] QI, H. – TIAN, W. – ZHANG, H.: Modelling Local Scour around A Cylindrical Pier with Circular Collar with Tilt Angles (Counter clockwise around The Direction Of The Channel Cross-Section) in Clear-Water, Water 13, 2021.

[18] MELVILLE, B.W. – COLEMAN, S.E.: Bridge Scour, Water Resources Publication, 2000.

[19] PAROLA, A. – HAGERTY, D. – MUELLER, D. – MELVILLE, B. – PARKER, G. – USHER, J.: The Need for Research on Scour at Bridge Crossings, Stream Stability and Scour At Highway Bridges: Compendium of Stream Stability and Scour Papers Presented at Conferences Sponsored By The Water Resources Engineering (Hydraulics) Division of The American Society Of Civil Engineers, 1997.

[20] SHIROLE, A. – HOLT, R.: Planning for a Comprehensive Bridge Safety Assurance Program, Transportation Research, 1991, pp. 290–305.

[21] RISK I. D.: Assessment of Existing Bridge Structures, University Of Cambridge, 2004.
[22] IQBAL, A. – REHMAN, H.S.U. – MUNIR, M. – ASHIQ, M. – OMAR, A. – HAIDER, Z. – AKHTAR, M. – JAVED, M. – REHMAN, O. U. U. – ADNAN, M. – JAHANZAIB, M.: Time and Cost Overrun in Construction Projects of Pakistan, Pakistan Journal of Engineering and Technology, 2019, Vol. 2, pp. 22–29.
[23] IQBAL, A. – YOUSUF, M. – ULLAH, K. – ADNAN, M. – AHMAD, M. – ASHIQ, M. – SHEHZAD, U. – MUNIR, M. – REHMAN, S. U. – AKHTAR, M. – RIZWAN, M. – JAVED, M. – AKRAM, U.: Utilization of Waste Plastic Polymers to Improve the Performance of Modified Hot Mix Asphalt, Pakistan Journal of Engineering and Technology, 2020, Vol. 3, pp. 162–171.
[24] JAHANZAIB, M. – IQBAL, A. – ASHFAQ, H. – MUNIR, M. – AKHTAR, M. – ASHIQ, M. – IBRAHIM, B.: Partial Replacement of Coarse Aggregate By Using Pumice Aggregate in Lightweight Concrete experimental Investigation, Pakistan Journal of Engineering and Technology, 2021, Vol. 4 pp. 27–30.
[25] ATAIE-ASHTIANI, B. – BARATIAN-GHORGHI, Z. – BEHESHTI A.: Experimental Investigation of Clear-Water Local Scour of Compound Piers, Journal of Hydraulic Engineering, 2010, Vol. 136, pp. 343–351.
[26] VEERAPPADEVARU, G. – GANGADHARAIAH, T. – JAGADEESH, T.: Vortex scouring Process around Bridge Pier with a Caisson, Journal of Hydraulic research, 2011, Vol.49, pp. 378–383.
[27] NIMBALKAR, P. T. – THORAT, S.S.: Experimental Study of Local Scour around Circular Compound Bridge Pier, International Journal of Science, Engineering and Technology, 2012, pp.2395-4752.
[28] NAZARI-SHARABIAN, M. – NAZARI-SHARABIAN, A. – KARAKOUZIAN, M. – KARAMI, M.: Sacrificial Piles as Scour Countermeasures in River Bridges A Numerical Study Using Flow-3D, Civil Engineering Journal, 2020, Vol. 6, pp. 1091.
[29] GHASEMI, M. – SOLTANI-GERDEFARAMARZI, S.: The Scour Bridge Simulation around A Cylindrical Pier Using Flow-3D, Journal of Hydro sciences and Environment, 2017, Vol. 1, pp. 46–54.
[30] MENDONCA, I.S.P. – CANILHO, H.D.L. – FAEL, C.M.S.: Flow-3D Modelling of the Debris Effect on Maximum Scour Hole Depth At Bridge Piers, 38th Lahr World Congress, 2019, pp. 2813–2821.
[31] JALAL, H.K. – HASSAN, W.H.: Three-Dimensional Numerical Simulation of Local Scour around Circular Bridge Pier Using Flow-3D Software, IOP Conference Series: Materials Science and Engineering, IOP Publishing, 2020.

[32] SADAT HELBAR, M. – PARVARESH RIZI, A. – FARHOUDI, J. – MOHAMMADI, A.: 3D Flow Simulation to Improve the Design and Operation of The Dam Bottom Outlets, Arabian Journal of Geosciences, 2021, Vol. 14, pp. 1–11.
[33] SAJA I. A.: Experimental Investigation of Temporal Variation of Local Scour at Non-Uniform Piers", M.Sc. Thesis, University of Basrah, College of Engineering, Department of Civil Engineering, 2019.
[34] DAKHEEL, A. A. – AL-ABOODI, A. H. – ABBAS S. A.: Investigation for Hydrodynamic Processes Of Water in Khour Al-Zubair Port Using Hydrodynamic Model, Materials Today: Proceedings, 2022 Vol. 61, pp. 1073-1082
[35] CHEREMISINOFF, N. P. – GUPTA, R.: Handbook of Fluids and Motion, Butterworths, Boston, 1983.
[36] KOMBIADOU K. – KRESTENITIS Y. N.: Modelling Cohesive Sediment Dynamics in the Marine Environment, Chapter in Sediment Transport Processes and Their Modelling Applications, 2013, Manning A. J. (Eds.), Intech Open, pp: 213-246.
[37] Dakheel, A. A.: Modelling of Sediment Transport in Khour Al Zubair Port, South of Iraq", Ph.D. thesis, University of Basrah, College of Engineering, Department of Civil Engineering, 2022.
[38] Abdulhussein, I. A. – Qasim, R. M.: Pier scouring reduction using a Strip Guide Flow Panel device, RUDN Journal of Engineering Researches, 2019, Vol. 20, pp. 229–235.
[39] APSILIDIS, N. – ASCE, S.M. – Diplas, P. – ASCE, M. – Dancey, C.L. – Vlachos, P.P. – Raben, S.G.: Local Scour at Bridge Piers: The Role of Reynolds Number on Horseshoe Vortex Dynamics, International Conference on Scour and Erosion, (ICSE-5), Scour and Erosion, 2010.